A Control Methodology for Renewable Energy Integrations in Distribution Systems

M. J. Hossain, *Member, IEEE*, T. K. Saha, *Senior Member, IEEE*, and N. Mithulananthan, *Senior Member, IEEE*

***Abstract*-- This paper presents a systematic control methodology for intermittent renewable energy integrations in low voltage distribution systems considering operating constraints and limits. An output feedback decentralized controller is synthesized for renewable generators using a linear quadratic robust control strategy. The change in volatile renewable generations is considered as an uncertain term in the design algorithm. The designed controller, for both wind and photovoltaic (PV), ensures both steady state and transient voltage stability for a given integration level. Effectiveness of the proposed controller is verified on a 43 bus industrial mesh distribution system under large disturbances and it is found that the designed control scheme enhances the stability and making the renewable integration grid friendly.**

***Index Terms*-- Distributed Generations, Voltage Constraints, Decentralized Control and Generation and load uncertainties.**

I. NOMENCLATURE

Symbols in the order in which they appear

R_s: Stator resistance	R_s, R_{sh}: series & shunt resistances
L_s: Stator inductance	α: firing angle of PWM scheme
ω: synchronous speed	K: amplitude modulation index
v_{ds}: d-axis stator voltage	i_{pv}: current flowing through array
v_{ds}: q-axis stator voltage	v_{pv}: output voltage of array
i_{ds}: d-axis stator current	R_{dc}, L_{dc}, C_{dc}: resistance, reactance and capacitance of DC-link
i_{ds}: q-axis stator current	i_{dc}: Current flowing through DC-link,
ψ : magnet flux	R_{out}, L_{out}: Resistance and reactance of the line connected to the grid
H_{tot}: inertia constant	i_{out}: Current flowing through the line connected to the grid
T_M: mechanical torque	q: Charge of electron
T_e: electromagnetic torque	T: Temperature
i_{DQg}: dq axis currents of the grid-side converter	x: state vector
v_{DQg}: dq axis voltages of the grid-side converter	u: Control input
v_{DC}: DC Capacitor voltage	y: Measured output
i_{DC}: current through capacitor	ζ: Uncertainty output
C: Capacitance	ξ: Uncertainty input
I_{ON}: dark diode characteristics of photocells	A,B,C,D: System matrices
I_L: light-generated current	τ, θ: free parameters
L_{pv}, C_{pv}: wiring inductance and capacitance	
I_s: saturation current	

This work was supported by the CSIRO Australia under Intelligent Grid Flagship Project.

The authors are with the School of ITEE, University of Queensland, St. Lucia, Brisbane, QLD 4072, Australia. e-mail: m.hossain9@uq.edu.au and (saha, mithulan)@itee.uq.edu.au.

II. INTRODUCTION

The installed capacity of DG with wide range of technologies is expected to continue to increase over the coming years in order to meet the 21st century electricity demand [1]. The technologies of DG include wind turbines, small hydro turbines, combine heat and power (CHP) units, photovoltaic (PV) and fuel cells. Due to the wide variety of technologies the integration of small, decentralized power generators brings both positive and negative impacts and technical challenges to the power grid. These technical challenges have to be resolved for getting benefits from interconnection of wide-scale DG to the existing grids. Implementation of appropriate control for DG units based on their technology can improve the performance of DG units without violating network constraints; facilitate the effective participation of DG and its penetration.

Voltage rise is one of the key technical challenges limiting the amount of additional DG capacity that can be connected to rural distribution networks. Moreover transient voltage variation in the form of oscillation with increase in amplitude and dynamic voltage stability can limit the DG penetration [2]. The large-scale penetration of DG also has an impact on the short-term stabilities (voltage and transient) of a system and, when it increases, its impact is no longer restricted to the distribution network but begins to influence the entire power system [3] by either improving or deteriorating its stability performance.

Different control systems for accommodating DG in the network are currently being investigated. They aim to improve the performance of DG units and hence the distribution system without violating network constraints, and provide appropriate frameworks for them to participate effectively in the power system. Two different control levels have been identified, the DG unit and distribution network levels. Moreover, a number of control paradigms for providing the framework required for the operation and management of distributed energy resources (DER) are also being investigated. A new voltage control procedure that includes optimizing only the steady-state operating conditions by using DG installed at the MV level, with microgrid and OLTC transformer control capabilities, is proposed in [5]. The authors in [6] present a comparison between the centralized and distributed approaches for controlling distribution network voltages in terms of the capacity of DG that could be accommodated within existing networks as well as contrasting them with the current power factor control approach. However, in both [4] and [6], the

controllers are designed to satisfy the steady-state requirements of the systems and the system dynamics are not considered. As under certain operating conditions the integration level is limited by the transient and voltage stabilities [7], advanced control can enhance penetration level [8]. To date, in the literature, the control objective has been focused on the steady-state control of a distributed system. However, as stated above, for large-scale DG integration, the penetration level can be limited by transient voltage variations and dynamic voltage instability.

The secured operation of the distribution system strongly depends on the performance of the control system. Most of the DG units have more intermittent characteristics and less inertial response. They are connected to grids through power electronics converters which are very sensitive to grid disturbances. Therefore, it is important that the designed controllers should be robust and guarantee stability under any faults and load variations. This paper presents a new decentralized control for robust DG integration that ensures stability during large disturbances without violating grid codes and system constraints. Changes in DG penetration are considered with uncertainty in the system model and the controller is synthesized via optimization of the worst-case quadratic performance of the underlying uncertain system. In addition, the interconnection effects of other subsystems are considered in designing the control, which enhances the robustness of the closed loop system.

The organization of the paper is as follows: Notation and symbols used throughout the paper is listed in Section I and Section II explains the motivation and current state of the art in control of DG. Section III provides the mathematical modeling of distribution system, including distributed generators. Test system and control objectives are presented in Section IV. Section V describes the decentralized output-feedback controller design procedure and Section VI depicts the control design algorithm. The performance of the controller is outlined through a series of nonlinear simulation results and is presented in Section VII. Concluding remarks and suggestions for future works are given in Section VIII.

III. POWER SYSTEM MODELING

In this paper, we consider three different types of DG units: (i) direct-drive wind generator (DDWGs); (ii) doubly-fed induction generators (DFIGs); and (iii) PV generators. The main grid is represented as an infinite bus. Fig. 1 shows a simple diagram of a DDWG system. The AC power output from the generator is converted into DC power through rectifier circuits. The grid-side connection is realized by a self-commutated pulse-width modulated (PWM) converter that imposes a pulse-width modulated voltage to the AC-terminal.

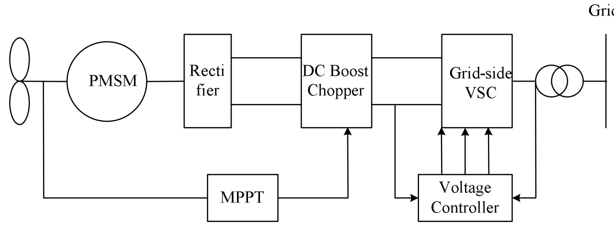

Fig. 1 Schematic diagram of DDWG.

This direct-drive permanent magnet synchronous generator uses constant excitation. The dynamic model of the DDWG can be described given by equations (1)-(4) [9]:

$$L_s \frac{di_{ds}}{dt} = -v_{ds} - R_s i_{ds} + L_s \omega i_{qs} \quad (1)$$

$$L_s \frac{di_{qs}}{dt} = -v_{qs} - R_s i_{qs} - L_s \omega i_{ds} + \omega \psi \quad (2)$$

As the permanent generator is directly connected to the turbine, the model of the drive train can be represented by the one-mass model given by:

$$H_{tot} \frac{d\omega_t}{dt} = T_M - T_e \quad (3)$$

The DDWG is connected to the grid via a full-scale back-to-back converter. The active power flow through the converter is balanced via the DC link which is modeled as:

$$Cv_{dc} \frac{dv_{dc}}{dt} = v_{Dg} i_{Dg} + v_{Qg} i_{Qg} + v_{ds} i_{ds} + v_{qs} i_{qs} \quad (4)$$

The nonlinear model of a DFIG is mainly based on a static model of the aerodynamics, a two-mass model of the drive train and a third-order model of the generator. It also includes a grid-side converter (GSC), a DC-link capacitor, a pitch controller and a rotor-side converter (RSC).

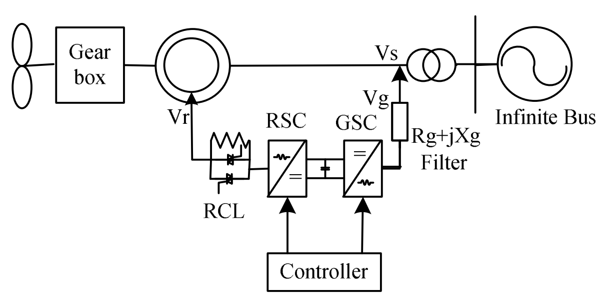

Fig. 2. Schematic diagram of DFIG.

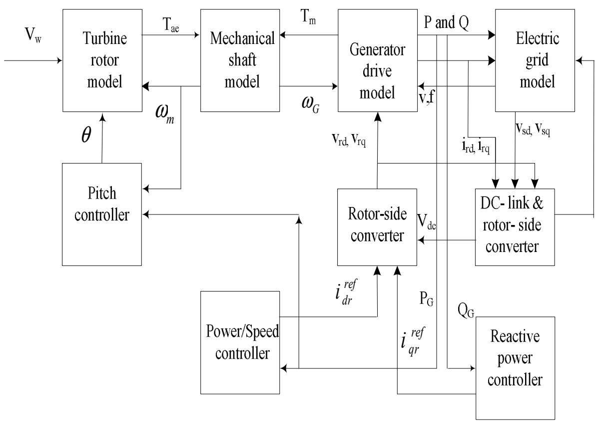

Fig. 3. Block diagram of DFIG wind generation system.

A typical scheme of a DFIG-based wind turbine is shown in Fig. 2, in which its stator is connected directly to the grid and rotor is connected through two voltage-fed PWM converters and rotor current limiter (RCL). The power flow between the rotor and grid can be controlled both in magnitude and direction. The corresponding block diagram for DFIG modeling is shown in Fig. 3. A two mass model of the drive train [10], third order model of the generator [11] and a first order model of the converter [12] are used in this paper.

A PV array system connected to the grid through a DC-AC inverter, a DC-DC converter and a DC-AC converter. As, generally, the output voltage of a PV module is low, at first a DC-AC converter is used to convert the output of the PV array into AC which is then stepped up through a transformer. Again, AC is converted into DC and transmitted through the DC link to reduce its loss. Therefore, it can be said that a DC-AC-DC converter operated at 50 Hz is used to increase the voltage level as per grid requirements.

The equivalent circuit of a PV system is shown in Fig. 4. The dynamic model, described in [13] and [14], is used in this research.

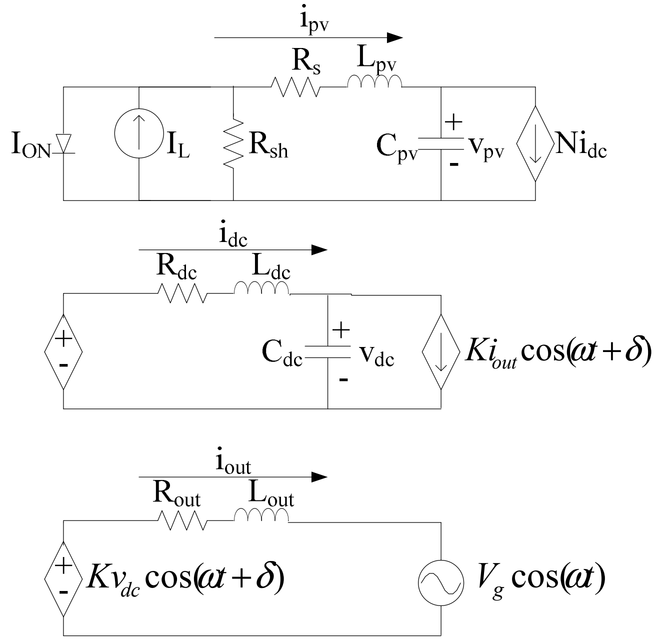

Fig. 4 Equivalent circuit diagram of grid-connected PV system.

IV. Test System and Control Strategy

A 43-bus industrial meshed system is used in this paper [15]. A single-line diagram of it is shown in Fig. 5 and the numerical values of its parameters are given in [15]. It is modified by connecting two wind farms at buses 39 (DFIG) and 50 (DDWG) and a PV generator at bus 4. There are five different voltages are available: 69kV, 13.8kV, 4.16kV, 2.4kV and 0.48kV, in the test distribution system. In the original system the two plant generators at buses 4 and 50 supply 87% of the real power load, with the remainder coming from main grid through the substation located at bus 100. It is a meshed distribution system with a total load of 21.76 MW and 9 MVAr which is modeled as (i) a 80% induction motor load [16] and (ii) a 20% static load. To study this, the test system is stressed by increasing the load demand to twice those given in [15].

A. Control strategy for renewable generators

In this paper, a decentralized control for DG accommodation is proposed where the system includes DFIGs, DDWGs and PV generators. The controllers for both GSC and RSC of a DFIG are shown in Fig. 6(a) in which P_g represents the real power output, Q_g the reactive power, V_{dc} the DC-link voltage, v_t the terminal voltage, v_d and v_q the d and q-axis voltage,

respectively, subscripts r and g the rotor and grid, respectively.

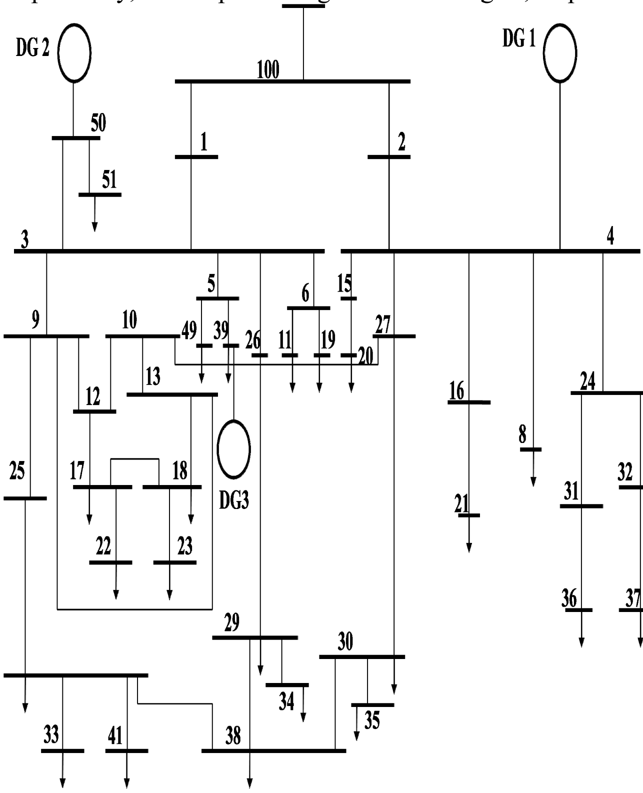

Fig. 5 Single line diagram of 43 bus test distribution system.

The function of the rotor-side converter control is to limit the rotor fault current and to increase the damping of stator flux, and consequently, to enhance the ride-through capability. The main objective of the GSC control is to keep the DC voltage constant and is to regulate the reactive current for controlling generator reactive power. Since the DC link dynamics is nonlinear, the conventional linear control cannot properly limit the DC voltage under severe voltage dips. Therefore, by using the proposed control approaches, the wind generator contributes to grid stability enhancement by controlling both active and reactive powers taking into account the nonlinearity of wind generators.

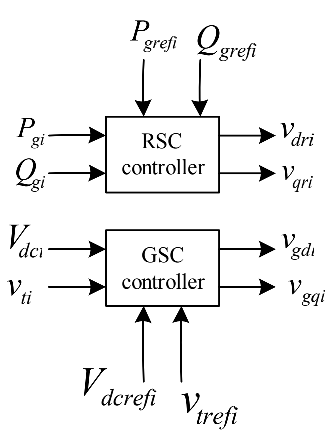

Fig. 6(a) Control strategy for DFIG.

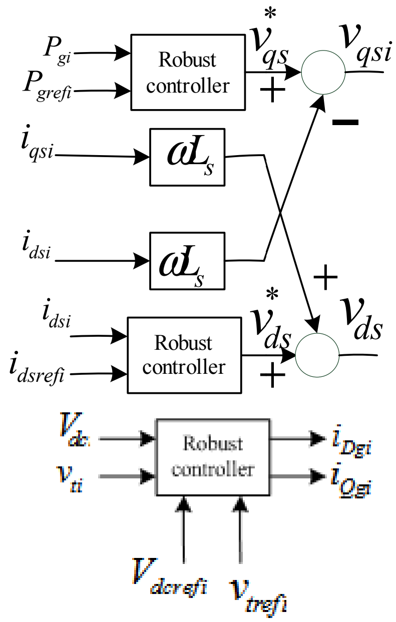

Fig. 6 (b) Generator-side converter control (upper one), GSC control (lower one) of DDWG.

The function of the generator generator-side converter of a DDWG, as shown in Fig. 6(b), is to control the output power to track the input of the wind input torque and minimize the power loss of the generator. On the other hand the grid-side converter control, as shown in Fig. 6(b), maintains the DC and

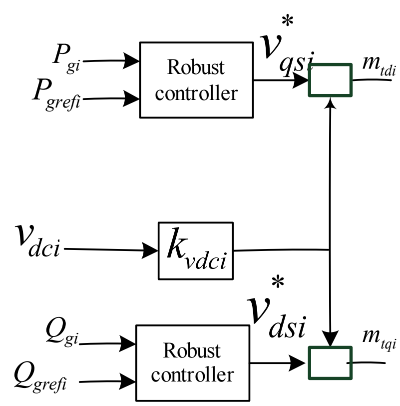

Fig. 6 (c) Control strategy for PV.

terminal voltages. In the voltage control mode of PV, P and Q are controlled, respectively, by the phase angle of and the amplitude of the VSC terminal voltage. The control strategy in *d-q* frame is shown in Fig. 6 (c).

V. Problem Formulation

The power system model used in this paper is described by the following large-scale system comprising N number of subsystems denoted by S_i, i=1,2, . . .N [17], [18], [19]:

$$S_i : \dot{x}(t) = A_i x_x(t) + B_i u_i(t) + +E_i \xi_i(t) + L_i r(t) \qquad [5]$$

$$z_i(t) = C_i x_x(t) + D_i \xi_i(t) \qquad [6]$$

$$\zeta_i(t) = G_i x_x(t) + H_i u_i(t) \qquad [7]$$
$$y_i(t) = C_{yi} x_x(t) + D_{yi} \xi_i(t) \qquad [8]$$

where $x_i \in R^{ni}$ is the state vector, $u_i \in R^{mi}$ the control input, $\xi_i \in R^{pi}$ the perturbation, $\zeta_i \in R^{hi}$ the uncertainty output, $z_i \in R^{qi}$ the controlled output, $y_i \in R^{gi}$ the measured output, and the input r_i describes the effect of the other subsystems ($S_1, \ldots, S_{i-1}, s_{i+1}, \ldots, S_N$) on subsystem S_i. The structure of system *is* shown in Fig. 7.

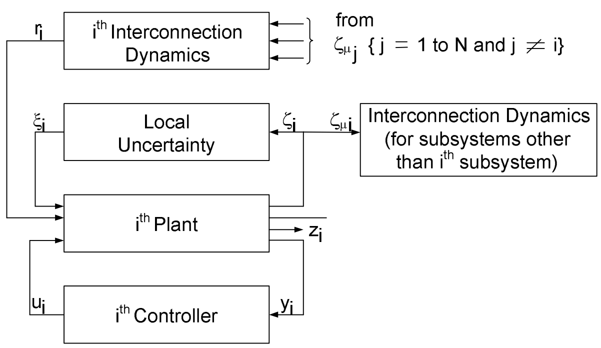

Fig. 7 Block diagram of decentralized control.

The system models (5) to (8) reflect the nature of a generic interconnected uncertain system in which each subsystem is affected by uncertainties that have two sources. Local uncertainties in the large-scale system arise from the sudden change in generation. Such dynamics is driven only by the uncertainty output (ζ_i) of subsystem S_i. A second source of uncertainties arises from interactions between the subsystems of the large-scale system. Indeed, the partitioning of a complex uncertain system into a collection of subsystems (S_i) results in the uncertainty in the original system being distributed among the subsystems. This provides the motivation for treating the interconnections as uncertain perturbations.

The power system under consideration satisfies the assumptions of: (i) $D_i^T D_i + G_i^T G_i > 0$ and $D_{yi} D_{yi}^T > 0$; (ii) the pair $(A_i,\, C_i^T C_i)$ is observable; and (iii) the pair $(A_i,\, B_i^T B_i)$ is able to be stabilized.

We define $\zeta_i = \Delta_i \xi_i$ and $r_i = \Delta_{ij} \xi_i$ where Δ_i and Δ_{ij} are the uncertain gain matrices. The uncertainty and interconnection must satisfy the following conditions:

$$\|\zeta_i\|^2 \le \|\xi_i\| \text{ and } \|r_i\|^2 \le \|\xi_i\|. \qquad (9)$$

The minimax output-feedback controller designed in this paper minimizes the following cost subject to the above (27) bounds on the local uncertainty and interconnections, $\|\zeta_i\|^2 \le \|\xi_i\|$. Associated with the uncertain system (23) to (26), we consider a cost functional of the form:

$$\int_0^\infty \sum_{i=1}^{N} \|z_i(t)\| dt \qquad (10)$$

The minimax optimal control finds the controller which minimizes the above cost function over all admissible uncertainties which satisfy the following relationship:

$$\inf_{u_i,\ i=1\ldots N} \sup_{\Xi,\Pi} \int_0^\infty \sum_{i=1}^{N} \|z_i(t)\| dt \le \inf_{\Gamma} \sum_{i=1}^{N} x_{i0}^T [X_i + \tau_i M_i + \theta_i \overline{M}_i] x_{i0} \qquad (11)$$

where $[x_{i0} \ldots\ldots x_{N0}]$ is the initial condition vector, Ξ a set of all admissible uncertainties and Π a set of interconnection inputs, $\Gamma = \{\{\tau_i, \theta_i\}_{i=1}^{N} \in R^{2N}\}$, a set of vectors, and $M_i > 0$ and $\overline{M}_i > 0$ two positive definite symmetrical matrices. Matrices X_i and Y_i are the solutions to the following pair of parameter-dependent coupled algebraic equations [18]:

$$A_i^T Y_i + Y_i A_i + Y_i \overline{B}_{2i} \overline{B}_{2i}^T Y_i - [C_{yi}^T W_i^{-1} C_{yi} - \overline{C}_i^T \overline{C}_i] = 0, \qquad (12)$$

$$A_i^T X_i + X_i A_i + \overline{C}_i^T \overline{C}_i - X_i [B_i R_i^{-1} B_i^T - \overline{B}_{2i} \overline{B}_{2i}^T] X_i = 0, \qquad (13)$$

where $R_i = \overline{D}_i^T \overline{D}_i$, $W_i = \overline{D}_{yi} \overline{D}_{yi}^T$ and $\overline{\theta}_i = \sum_{n=1,\, n \ne i}^{N} \theta_n$,

$$\overline{C}_i = \begin{bmatrix} C_i \\ (\tau_i + \overline{\theta}_i)^{1/2} H_i \end{bmatrix},\quad \overline{D}_i = \begin{bmatrix} D_i \\ (\tau_i + \overline{\theta}_i)^{1/2} G_i \end{bmatrix},$$

$$\overline{B}_{2i} = [\tau_i^{-1/2} E_i \quad \theta_i^{-1/2} L_i],\quad D_{yi} = [\tau_i^{-1/2} D_{yi} \quad 0].$$

These solutions are required to satisfy the following conditions:

$\tau_i > 0$, $\theta_i > 0$, $X_i \ge 0$, $Y_i \ge 0$ and $Y_i > X_i$.

Then, the controller is designed using the equations 18]:

$$\dot{x}_{ci} = \{A_i - [B_i R_i^{-1} B_i^T - \overline{B}_{2i} \overline{B}_{2i}^T] X_i\} x_{ci} + [Y_i - X_i]^{-1} C_{yi}^T W_i^{-1} [y_i(t) - C_{yi} x_{ci}] \qquad (14)$$

$$u_i = -R_i^{-1} B_i^T X_i x_{ci}. \qquad (15)$$

VI. CONTROL ALGORITHM

In this paper, a controller for accommodating DG units that ensure dynamic stability and provide required steady-state voltage is designed. The test system is divided into three subsystems: (i) a DFIG; (ii) a DDWG; and (iii) a PV. A controller is designed for each subsystem. The structure of the control is shown in Fig.7 and the control design algorithm is implemented in the following steps:

Step 1: solve the base case's power flow and monitor bus voltages;
Step 2: linearize the complete dynamic system about the desired equilibrium point: one part consists of the states of the devices in the subsystem (x_i) and the other with the rest of the states (r_i); *the m*atrices A_i and L_i are appropriately chosen from the complete linearized model equations; and then determine the other matrices given in the problem formulations in Section V corresponding to the control input, measured output and control variable;
Step 3: increase the generation profile, perform a power flow and check the bus voltage again; if the bus voltage is within the statutory limit (±10% of nominal voltage), go to next step, otherwise go to (ix);
Step 4: obtain the uncertain matrix (E_i) taking the difference between the matrices of subsystem A_i for the nominal and the increased generations;
Step 5: solve the optimization problem using the line search technique for the positive values of τ_i and θ_i which can be achieved by the MATLAB function *fmincon* with a proper initialization;
Step 6: substitute the values of τ_i and θ_i and solve the Riccati equations given in (12) and (13);
Step 7: design the controller according to (14) and (15); if a feasible controller is obtained, go to next step, otherwise go to (x);
Step 8: perform a time-domain simulation and evaluate the controller's performance for the worst case scenario;
Step 9: if the controller satisfies both the static and dynamic constraints, go to (ii), otherwise (ix); and
(x) stop and specify the upper level of DG integration.

VII. CONTROLLER PERFORMANCE EVALUATION

The upper levels of DG penetration using the above mentioned procedure are given in Table I. The output powers of all generators are increased simultaneously in order to determine the upper level. To assess the performance of the designed controller, the integration level using a conventional PI controller is also determined. From Table I, it is clear that the designed controller can accommodate more DG compared to the conventional PI controller; for example, at bus 50 integration level can be enhanced by 13.63% with the robust control. The upper level is determined based on the grid codes, i. e., steady state voltage remains within ±10% of the nominal voltage, transient voltage restores within 2 s and minimum damping of critical mode is 5%.

To verify the robustness performance of the designed controller, a number of cases are carried out and compared the performance of the designed controller with PI controller under different operating conditions, such as: (i) sudden change in generations, (ii) severe three-phase fault and (iii) permanent change of connected load.

Firstly, the controller's performance is verified with the upper integration level using the PI control, i.e., DG_1=15.25 MW, DG_2=16.5MW and DG_3=20 MW as given in Table I, for a sudden temporary change in generation. Figs. 11 and 12 show the real power output and terminal voltage response of the DFIG for a sudden 20% change in output real power. From Figs. 12 and 13 it is clear that, although both controllers ensure stable operation, the designed controller provides better performance in terms of damping, oscillations and settling time. The real power and voltage restores to the pre-fault value within 0.5 s compared to 6 s with the PI control.

TABLE I: PENETRATION LEVELS (MW)

Control	Bus 4 PV	Bus 50 DDWG	Bus 39 DFIG
PI	15.25	16.5	20
Robust	16.75	18.75	23.5

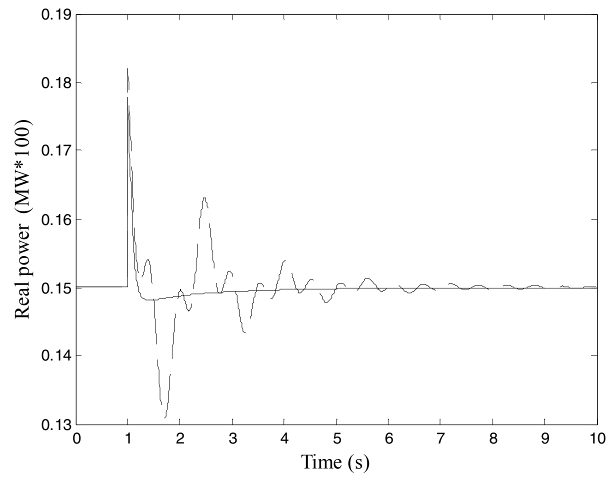

Fig. 11 Real power of DFIG for a sudden change in generation (solid line proposed control and dotted line PI).

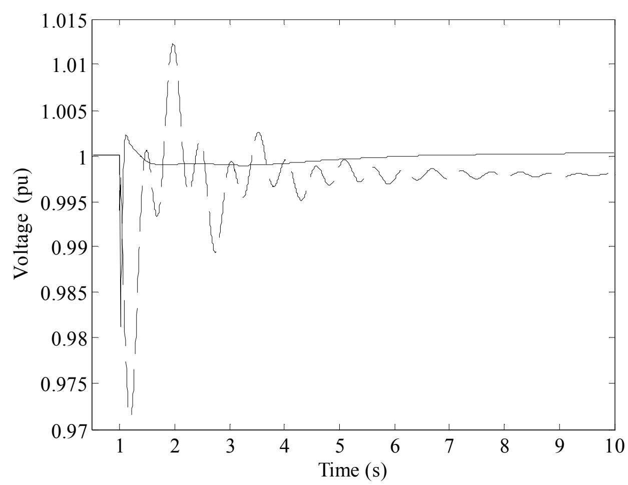

Fig. 12 Terminal voltage of DFIG for a sudden change in generation (solid line proposed control and dotted line PI).

The performance of the controller is also verified under a severe three-phase fault. A symmetrical three-phase fault is applied on bus 31 at 1 s and cleared after 0.2 s. Figs. 13 and 14 show the output power and terminal voltage of the DFIG using both the proposed robust control and the conventional control from which it is clear that tuned PI (trial and error method) control produces oscillatory behaviors. From modal analysis,

it is found that the oscillation occurs due to the interactions among different controllers and the critical modes are control modes. However, the robust performance of the designed controller ensures grid standards and utility requirements.

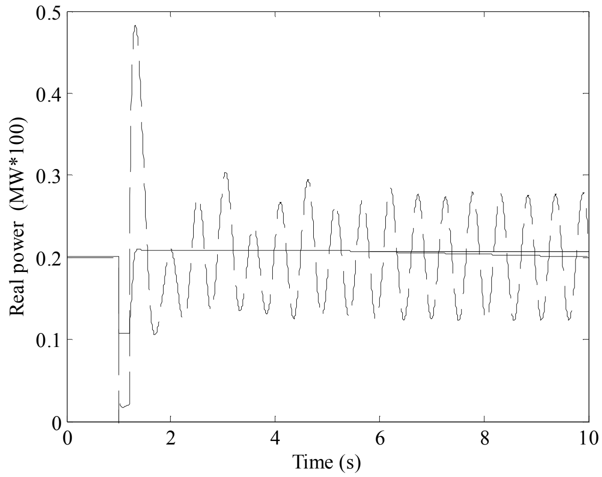

Fig. 13 Real power of DFIG for three-phase fault (solid line proposed control and dotted line PI).

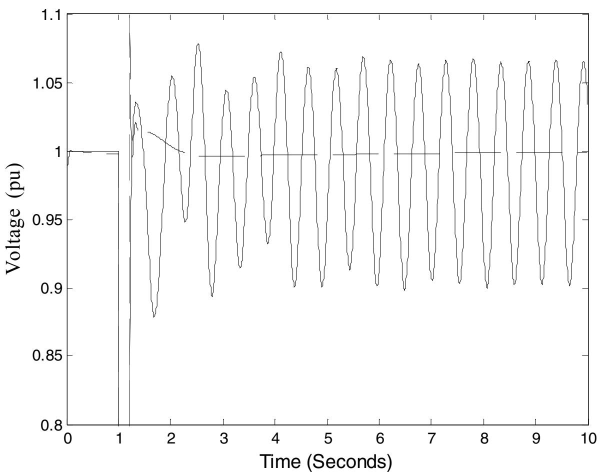

Fig. 13 Terminal voltage of DFIG for three-phase fault (solid line proposed control and dotted line PI).

Although the controller is designed for rated operating conditions, the designed controller performs well in different loading conditions. This is due to the incorporation of uncertainties in the design of the controller and the control algorithm proposed in this research ensures stability as long as condition (11) holds. Figs. 14 and 15 show the PCC voltage and real power output due to the 10% increase in load from which it is clear that the controller stabilizes the system at different equilibrium point.

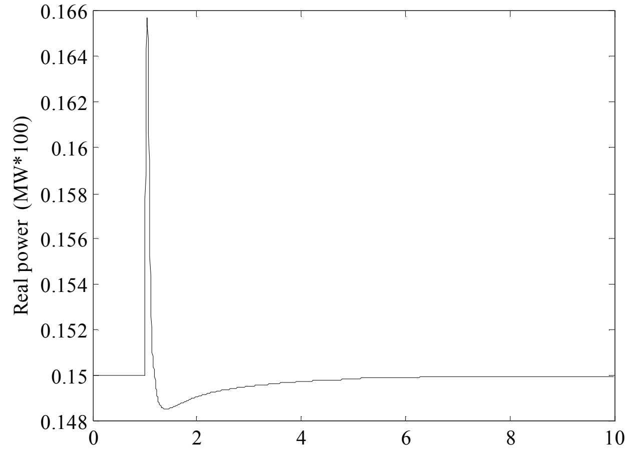

Fig. 14 Real power output of DDWG due to 10% change in load.

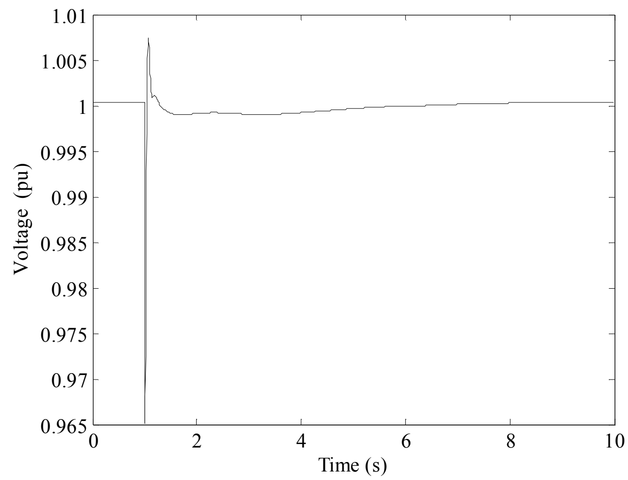

Fig. 15 Real power output of DDWG due to 10% change in load.

VIII. CONCLUSION

A systematic robust control methodology for intermittent and volatile renewable generation integration into existing grids is presented in this paper. Control strategies for different types of renewable generators are discussed in detail. It is found that transient voltage instability can limit DG penetration in weakly coupled system although voltage rise is a major constraint when accommodating DG units. The proposed controller ensures stability in the presence of generation uncertainty, interconnection effects and less inertial weekly coupled generators. From the simulation results, it is shown that the proposed robust control method can augment the potential penetration of DG units without requiring network reinforcements or violating a system's operating constraints.

REFERENCES

[1] T. Ackermann, G. Andersson, and L. Soder, “Distributed generation: a definition,” *Electric Power Systems Research, vol. 57, no 3, pp. 195-204, April 2001*.

[2] J. A. Pecas Lopes, N. Hatziargyriou, J. Mutale, P. Djapic and N. Jenkins, “Integrating distributed generation into electric power system: A review of drivers, challenges and opportunities,” Electric Power Systems research, vol. 77, no. 9, pp. 1189-1203, July 2007.

[3] M. Reza, J. G. Slootweg, P. H. Schavemaker, W. L. Kling and L. van der Sluis, “Investigating impact of distributed generation on transmission system stability,” in *IEEE Bologna Power Tech Conference,* Bologna, Italy, 23-26 June 2003, pp. 1-7.

[4] A.G. Madureira and J.A.Pecas Lopes, “Coordinated voltage support in distributed networks with distributed generation and microgrids,” *IET Renewable Power Generation,* vol. 3, no. 4, pp. 439-454, December 2009.

[5] P. N. Vovos, A. E. Kiprakis, A. Robin and G. P. Harrison, “Centralized and distributed voltage control: impact on distributed generation penetration,” *IEEE Trans. on Power Systems*, vol. 2, no. 1, pp. 476-483, February 2007.

[6] B. Meyer, Y. Bamberger and I. Bel, “Electricité de France and integration of distributed energy resources,” *IEEE Power Engineering Society General Meeting*, Montreal, Que, 18-22 June, 2006, pp. 1-6.

[7] B. L. Schenkman, D. G. Wilson and R. D. Robinett, “Photovoltaic distributed generation for Lunai power grid real-time simulation and control integration scenario,” International *Symposium on Power Electronics, Electrical Drives, Automation and Motion,* Pisa, 14-16 June, 2010, pp-154-157.

[8] J. Hiscock, N. Hiscock and A. Kennedy “Advanced voltage control for networks with distributed generation,” *9th International Conference on Electricity Distribution*, Vienna, 21-24 may 2007, pp. 148-151.

[9] F. Wu, X.-P. Zhang and P. Ju, “Modeling and control of the wind turbine with the direct drive permanent magnet generator integrated to power grid,” in *Third International Conference on Electric Utility Deregulation and Restructuring and Power technologies* , Nanjing, China, 6-9 April 2008, pp. 57-60.

[10] T. Ackermann, Wind Power in Power Systems. England; John Willey and Sons, Ltd, 2005.

[11] Y. Lei, A. Millane, G. Lightbody and K. Yacamini, “Modeling of the wind turbine with a doubly fed induction generator for grid integration studies,” *IEEE Trans. on Energy Conversion*, vol. 21, no. 1, pp. 257–264, March 2006.

[12] M. Rahimi and M. Parniani, “Coordinated control approaches for low-voltage ride-through enhancement in wind turbines with doubly fed induction generators,” *IEEE Trans. on Energy Conversion.*, vol. 25, no. 3, pp. 873–883, September 2110.

[13] A. Yazdani, A. Rita Di Fazio, H. Ghoddami, M. Russo, M. Kazerani, J. Jatskevich, K. Strunz, S. Leva and J. A. Martinez, “Modeling guidelines and a benchmark for power system simulation studies of three-phase single-stage photovoltaic systems,” IEEE Trans. on Power delivery, vol. 26, no. 2, pp. 1247–1264, April 2011.

[14] C. Rodriguez and G. A. J. Amaratunga, “Dynamic stability of grid-connected photovoltaic systems,” in *IEEE Power Engineering Society General Meeting,* Colorado, USA, 6-10 June 2004, pp. 1–7.

[15] “IEEE Standard for Interconnecting Distributed Resources with Electric Power Systems," IEEE std. 1547-2003, 2003.

[16] M. J. Hossain, H. R. Pota, V. Ugrinovskii and R. A. Ramos, “Voltage mode stabilization in power systems with dynamic loads,” *International Journal of Electrical Power & Energy Systems*, vol. 32, no. 8, pp. 911-920, November 2010.

[17] L. Li, V. A. Ugrinovskii and R. Orsi, “Decentralized robust control of uncertain markov jump parameter systems via output feedback,” *Automatica*, vol. 43, no. 11, pp. 1922-1944, November 2007.

[18] M. J. Hossain, H. R. Pota and C. Kumble, “Decentralized robust static synchronous compensator control to augment dynamic transfer capability,”, *Journal of Renewable and Sustainable Energy*, vol. 2, no. 2, pp. 022701(1)-022701(20), March 2010.

[19] M. J. Hossain, H. R. Pota, V. A. Ugrinovskii, and R. A. Ramos, “Decentralized control to augment LVRT capability of wind generators with STATCOM/ESS,” in *IEEE Power and Energy Society General Meeting*, Minneapolis, Minnesota, USA, 25-29 July, 2010, pp. 1–8.

IX. BIOGRAPHIES

M. Jahangir Hossain (M’10) was born in Rajshahi, Bangladesh, on October 30, 1976. He received the B.Sc. and M.Sc. Eng. degrees from Rajshahi University of Engineering and Technology (RUET), Bangladesh, in 2001 and 2005, respectively and Ph.D. degree from the University of New South Wales, Australia, all in electrical and electronic engineering.

He is currently working as a research fellow in the School of Information Technology and Electrical Engineering, University of Queensland, Australia. Previously he worked as a lecturer and assistant professor at RUET for six years. His research interests are power systems, wind generator integration and stabilization, voltage stability, micro grids, robust control, electrical machine, FACTS devices, and energy storage systems.

Tapan Kumar Saha (M’93, SM’97) was born in Bangladesh in 1959 and immigrated to Australia in 1989. He received B.Sc.Eng. Degree in 1982 from Bangladesh University of Engineering & Technology, Dhaka, Bangladesh, M.Tech. in 1985 from the Indian Institute of Technology, New Delhi, India and PhD in 1994 from the University of Queensland, Brisbane, Australia. Tapan is currently a Professor in Electrical Engineering in the School of Information Technology and Electrical Engineering, University of Queensland, Australia. Previously he has had visiting appointments for a semester at both the Royal Institute of Technology (KTH), Stockholm, Sweden and at the University of Newcastle (Australia). He is a Fellow of the Institution of Engineers, Australia. His research interests include condition monitoring of electrical plants, power systems and power quality.

Nadarajah Mithulananthan (SM’10) received his Ph.D. from University of Waterloo, Canada in Electrical and Computer Engineering in 2002. His B.Sc. (Eng.) and M. Eng. Degrees are from the University of Peradeniya, Sri Lanka, and the Asian Institute of Technology, Bangkok, Thailand, in May 1993 and August 1997, respectively. He has worked as an electrical engineer at the Generation Planning Branch of the Ceylon electricity Board, and as a researcher at Chulalongkorn University, Bangkok, Thailand.

Dr. Mithulan is currently a senior lecture at the University of Queensland (UQ), Brisbane, Australia. Prior to joining UQ he was associate Professor at Asian Institute of Technology, Bangkok, Thailand. His research interests are integration of renewable energy in power systems and power system stability and dynamics.